PNAS INAUGURAL ARTICLE | IMMUNOLOGY AND INFLAMMATION

The lncRNA LUCAT1 is elevated in inflammatory disease and restrains inflammation by regulating the splicing and stability of NR4A2

Tim Vierbuchen[a], Shiuli Agarwal[a], John L. Johnson[b], Liraz Galia[a], Xuqiu Lei[a], Karina Stein[c,d], David Olagnier[e], Karoline I. Gaede[d,f], Christian Herzmann[g], Christian K. Holm[e], Holger Heine[c,d], Athma Pai[h], Aisling O'Hara Hall[i], Kasper Hoebe[b], and Katherine A. Fitzgerald[a,1]

This contribution is part of the special series of Inaugural Articles by members of the National Academy of Sciences elected in 2021.

Contributed by Katherine A. Fitzgerald; received August 9, 2022; accepted November 22, 2022; reviewed by Jorge Henao-Mejia and Kathryn J. Moore

The nuclear long non-coding RNA LUCAT1 has previously been identified as a negative feedback regulator of type I interferon and inflammatory cytokine expression in human myeloid cells. Here, we define the mechanistic basis for the suppression of inflammatory gene expression by LUCAT1. Using comprehensive identification of RNA-binding proteins by mass spectrometry as well as RNA immunoprecipitation, we identified proteins important in processing and alternative splicing of mRNAs as LUCAT1-binding proteins. These included heterogeneous nuclear ribonucleoprotein C, M, and A2B1. Consistent with this finding, cells lacking LUCAT1 have altered splicing of selected immune genes. In particular, upon lipopolysaccharide stimulation, the splicing of the nuclear receptor 4A2 (NR4A2) gene was particularly affected. As a consequence, expression of NR4A2 was reduced and delayed in cells lacking LUCAT1. NR4A2-deficient cells had elevated expression of immune genes. These observations suggest that LUCAT1 is induced to control the splicing and stability of NR4A2, which is in part responsible for the anti-inflammatory effect of LUCAT1. Furthermore, we analyzed a large cohort of patients with inflammatory bowel disease as well as asthma and chronic obstructive pulmonary disease. In these patients, LUCAT1 levels were elevated and in both diseases, positively correlated with disease severity. Collectively, these studies define a key molecular mechanism of LUCAT1-dependent immune regulation through post-transcriptional regulation of mRNAs highlighting its role in the regulation of inflammatory disease.

interferon | lncRNA | splicing

Significance

Long non-coding RNAs (lncRNAs) are abundant in the human genome, yet, in contrast to proteins, only a small portion of lncRNAs have been functionally characterized. We further explore the molecular basis of LUCAT1-dependent regulation of the inflammatory response. In this study, we identify LUCAT1-binding proteins that are involved in splicing and processing of mRNAs including the anti-inflammatory NR4A2. LUCAT1 regulates splicing and stability of NR4A2 which contributes to the inhibitory effect of LUCAT1 on interferons and inflammatory cytokines. Finally, data from COPD and IBD patients indicate that LUCAT1 levels are elevated in these patient groups where expression is positively correlated with disease severity. Thus, LUCAT1 may serve as a diagnostic marker for inflammation and as a therapeutic target in the future.

The immune system has evolved to protect the host from infection. Dynamic changes in immune gene expression are coordinately regulated downstream of pattern recognition receptors, such as Toll-like receptors. Overexuberant-immune responses lead to chronic inflammatory diseases and profound tissue damage. Tight regulation of the immune response is therefore essential to maintain homeostasis. A complex regulatory system is in place to ensure appropriate activation of immunity and the timely resolution of inflammation to return responses to their preactivated state. In myeloid cells for example, a series of negative regulators are induced which terminate signaling pathways and gene expression. These include IκBα, a post-induction feedback regulator of NF-κB, as well as SOCS1, which terminates cytokine receptor signaling. Long non-coding RNAs (lncRNAs) also have immunoregulatory roles in the immune system (1–4). LncRNAs are dynamically regulated in myeloid cells activated through TLRs and other sensors. These ncRNAs lack protein- or peptide-coding capacity and can be distinguished from other non-coding transcripts, such as miRNA by lengths longer than 200 nucleotides (5). The total number of lncRNAs in the human genome can only be estimated, and to this date, the GENCODE annotation (version 40) lists about 18,000 lncRNAs.

Despite the abundance of these ncRNAs in the genome, the functional characterization of most lncRNAs remains elusive. Yet, several examples of lncRNAs with immunoregulatory functions have been described. For example, lncRNAs, such as lincRNA-Cox2 (6) and ROCKI (regulator of cytokines and inflammation) (7), are induced in response to Toll-like receptor stimulation where they regulate the expression of inflammatory response genes. Additional lncRNAs like Morrbid modulate the lifespan of short-lived myeloid cells, such as eosinophils (8), and MaIL1 which stabilizes OPTN a signaling protein in the Toll-like receptor 4 pathway (9). Recently, LUCAT1 was identified as an inducible lncRNA localized to the nucleus where it was shown to act as a negative feedback inhibitor of type I interferon (IFN) and inflammatory gene expression (10). Although these results indicated that LUCAT1 altered STAT1 binding to the promoters of interferon-stimulated genes (ISGs), the precise molecular mechanism of LUCAT1-dependent regulation of type I IFN and

Reviewers: J.H.-M., University of Pennsylvania; and K.J.M., NYU Langone Health.

Competing interest statement: The authors have research support to disclose. This work is supported by a sponsored research grant from Janssen Research and Development, LLC to K.A.F.)., Yes, the authors have public statements and positions to disclose. K.A.F. is a consultant for Janssen Pharmaceuticals and a recipient of a sponsored research agreement that covered part of this work.

[1]To whom correspondence may be addressed. Email: kate.fitzgerald@umassmed.edu.

This article contains supporting information online at https://www.pnas.org/lookup/suppl/doi:10.1073/pnas.2213715120/-/DCSupplemental.

Published December 28, 2022.

inflammatory cytokines, such as interleukin 6 (IL-6), remains unknown. Understanding how lncRNAs modulate target gene expression is facilitated by defining the proteins it interacts with. In this study, we characterized in detail the protein-binding partners of LUCAT1 in myeloid cells. We found that LUCAT1 is associated with RNA-processing factors which affect splicing. We identified altered splicing patterns of induced genes in LUCAT1-deficient cells. In particular, an anti-inflammatory gene, nuclear receptor 4A2 (NR4A2, also known as NURR1), previously linked to termination of NF-κB signaling was regulated at the level of splicing in LUCAT1-deficient cells leading to altered stability of this factor. In addition, we found that LUCAT1 levels are increased in patients suffering from chronic obstructive pulmonary disease (COPD) or inflammatory bowel disease (IBD) and the levels of LUCAT1 correlate with disease severity. LUCAT1 therefore may serve as a potential biomarker and therapeutic target.

Results

The lncRNA LUCAT1 Is Induced by lipopolysaccharide (LPS) as Well as by Inducers of nuclear factor erythroid 2-related factor 2 (NRF2). LUCAT1 is a rapidly induced nuclear-localized lncRNA induced via NF-κB downstream of TLRs (10). LUCAT1 was initially discovered in lung epithelial cells however, where it can be induced by cigarette smoke extract through activation of NRF2, a transcription factor important for protection from oxidative stress (11). Four-octyl itaconate (4-OI) is a cell-permeable derivative of the Krebs cycle metabolite itaconate that can activate NRF2 signaling by alkylating Keap1 (12). 4-OI is known to negatively regulate immune gene expression. These anti-inflammatory properties originate largely from the ability of 4-OI to activate NRF2 (13, 14) or lead to the induction of the activating transcription factor 3 (15). To determine whether 4-OI induces LUCAT1 expression in human myeloid cells, we treated monocyte-derived dendritic cells (moDCs) with LPS or 4-OI and analyzed LUCAT1 expression levels by qRT-PCR (Fig. 1*A*). After treatment with 4-OI, LUCAT1 was significantly upregulated in moDCs, albeit weaker than that induced by LPS stimulation. LUCAT1 expression was induced after 2 h and peaked at 8 h (Fig. 1*B*). In addition, two other electrophilic agents, di-methyl itaconate (DI) and sulforaphane (SP), which also activate NRF2 (16), were used to treat moDCs in combination with LPS or LPS and IFN-α (Fig. 1*C*). Treatment with SP also induced LUCAT1 expression while DI had minimal effect. Overall, 4-OI shows the

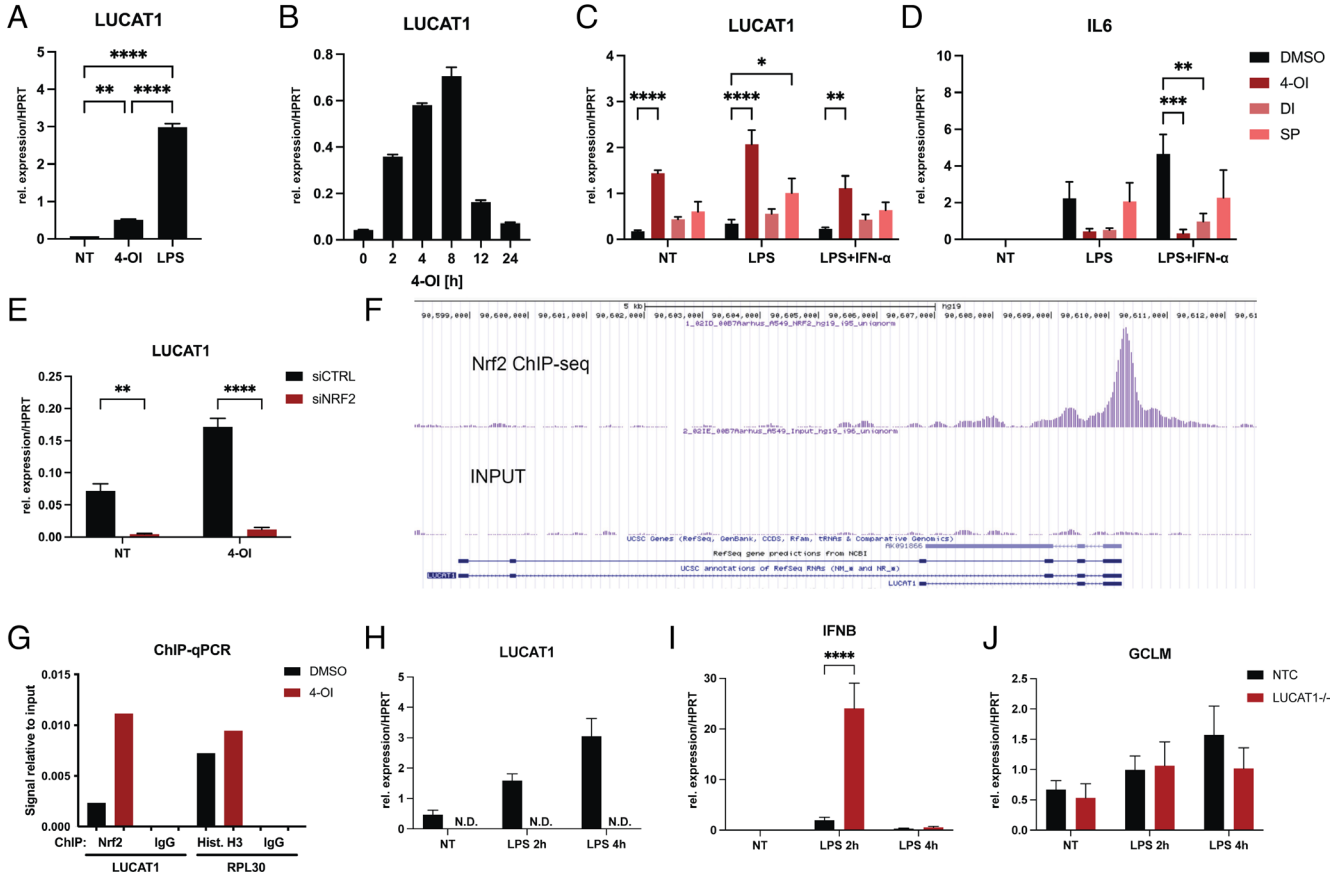

Fig. 1. LUCAT1 is induced by 4-octyl itaconate through an NRF2-dependent mechanism. (*A* and *B*) qPCR analysis of LUCAT1 expression in moDCs treated for 2 h with 100 μM 4-octyl itaconate (4-OI) or 200 ng/mL LPS in *A* and with 100 μM 4-OI for 0 to 24 h in *B*. Data are from three (*A*) or two (*B*) different healthy donors. (*C* and *D*) qPCR analysis of LUCAT1 (*C*) and IL6 (*D*) expression in moDCs pre-treated with 250 μM 4-OI, 250 μM di-methyl itaconate (DI) or 5 μM sulforaphane (SP) for 4 h before stimulated with 200 ng/mL LPS +/−10 ng/mL IFN-α 2b. Data are from three to four different healthy donors (n = 3 to 4). (*E*) qPCR analysis of LUCAT1 expression in MDMs pre-treated with control siRNA or siRNA for NRF2 and stimulated with 4-OI. Data are from three different healthy donors (n = 3). (*F*) ChIP-seq results from A549 cells for NRF2 in LUCAT1 locus. (*G*) ChIP-qPCR results from THP-1 cells showing amplification of LUCAT1 or RPL30 promoter region after pulldown with NRF2, Histone H3 or IgG control antibody precipitation. (*H–J*) qPCR analysis of LUCAT1 (*H*), IFNB (*I*), GCLM (*J*) expression in THP-1 control guide RNA (NTC) or LUCAT1$^{-/-}$ cells after stimulation with 200 ng/mL LPS for 2 or 4 h. Data are from four independent experiments (n = 4). (*A–H*) Data are represented as mean ± SEM. *P* values (*$P \le 0.05$, **$P \le 0.01$, ***$P \le 0.001$, ****$P \le 0.0001$) have been determined by one-way ANOVA in *A* or two-way ANOVA in *C–H*. NT: not treated; N.D.: not detectable.

most potent effect on LUCAT1 expression. Treatment of cells with these compounds also abrogated IL6 expression in LPS-stimulated conditions as expected (Fig. 1*D*).

To test whether the induction of LUCAT1 by 4-OI required NRF2, we treated NRF2-silenced monocyte-derived macrophages (MDMs) with the metabolite and measured LUCAT1 levels. Silencing of NRF2 reduced LUCAT1 expression levels even in the absence of 4-OI treatment (Fig. 1*E*). Similar results could be observed in the keratinocyte cell line HaCaT where 4-OI treatment failed to induce LUCAT1 when NRF2 was silenced (*SI Appendix*, Fig. S1). We also analyzed NRF2 chromatin immunoprecipitation (ChIP)-seq data in A549 cells, which supported binding of NRF2 in the LUCAT1 promoter region (Fig. 1*F*). Likewise, 4-OI treatment induced binding of NRF2 to the LUCAT1 promoter in THP-1 cells by ChIP-qPCR (Fig. 1*G*). Together these results demonstrate that LUCAT1 is induced by NRF2 in response to immunoregulatory metabolites, such as itaconate. We have previously shown that LUCAT-deficient cells have elevated TLR-induced IFN-β and inflammatory gene expression. We confirmed these observations by generating LUCAT1-deficient THP-1 cells, which had no detectable LUCAT1 expression after LPS treatment (Fig. 1*H*). LUCAT1-deficient THP-1 cells had markedly increased expression of IFN-β when stimulated with LPS (Fig. 1*I*). We also tested the expression of a known NRF2 target gene in these cells by measuring the levels of glutamate-cysteine ligase modifier subunit (GCLM). While the levels of this gene were only slightly elevated with LPS stimulation, we did not see any changes in GCLM expression in cells lacking LUCAT1 (Fig. 1*J*). Together therefore these observations indicate that LUCAT1 can be induced by TLR ligands as well as activators of NRF2; however, LUCAT1 does not appear to control NRF2 target genes in the LPS pathway.

Long-Read Nanopore Sequencing Identifies LUCAT1 Isoforms. We previously used rapid amplification of cDNA ends (RACE) and cloning to identify numerous different isoforms of LUCAT1 in LPS-stimulated DCs revealing a complex gene structure of the gene (10). To better define the LUCAT1 isoforms in moDCs, we utilized long-read sequencing (Oxford Nanopore) a long-read sequencing approach effective for the identification of transcripts, especially in the case of lncRNAs that are often not well annotated (17, 18). We sequenced moDCs and MDMs treated with LPS or the STING agonist diABZI-4 (19) and used the minimap2 and Stringtie software to align the reads and annotate potential transcripts (Fig. 2*A*). In accordance with our previous results, we found numerous isoforms of LUCAT1 with complex exon usage (*SI Appendix*, Fig. S2). Among the four most abundant isoforms was a transcript we named LUCAT1.1, that was characterized by

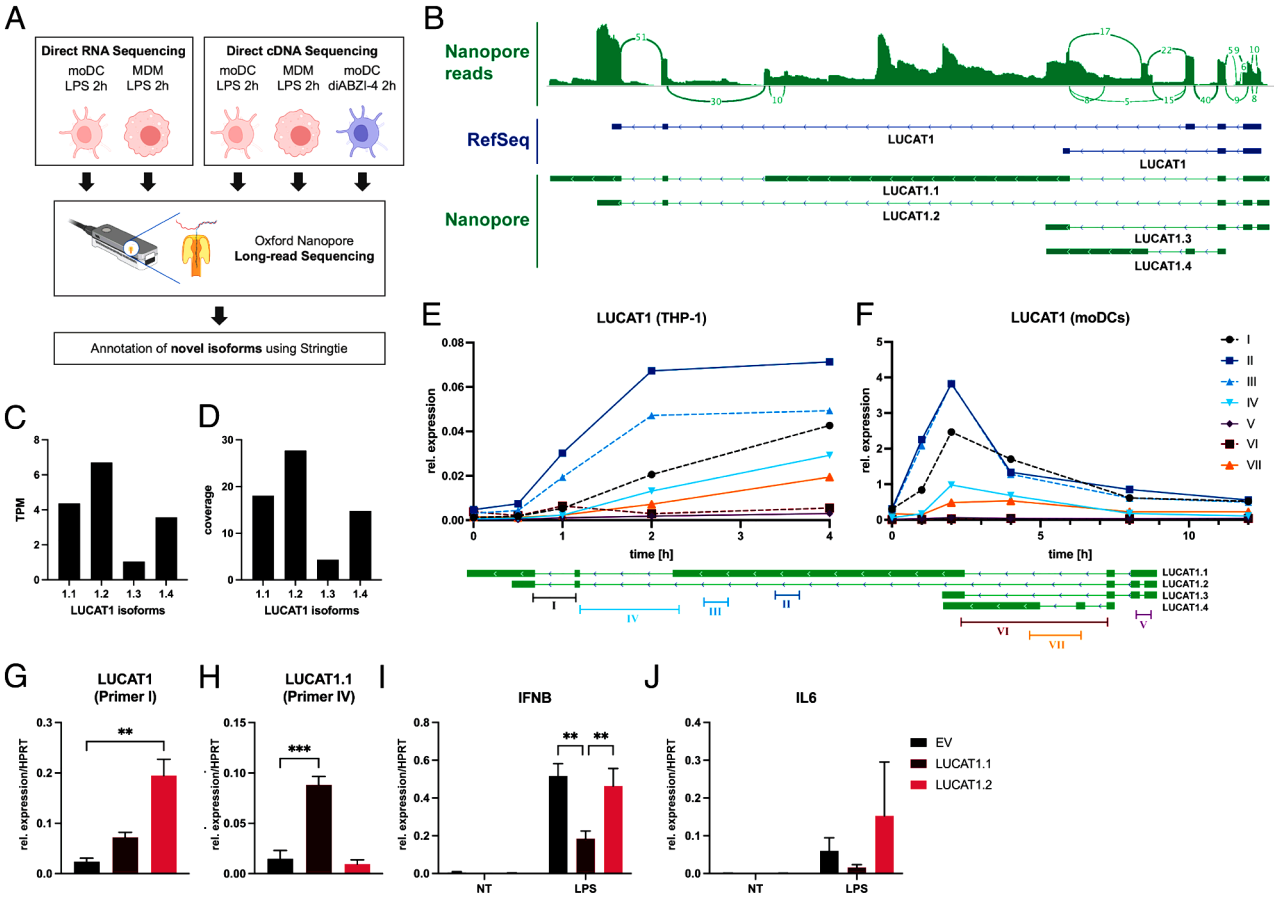

Fig. 2. LUCAT1 isoforms determined by long-read sequencing. (*A*) Schematic of long-read nanopore sequencing that was used to determine isoforms of LUCAT1. (*B*) Combined reads from sequencing (*Top*), reference annotation from RefSeq (*Middle*), and isoforms with highest expression levels from annotation based on sequencing results (*Bottom*). (*C* and *D*) TPM and coverage for isoforms shown in *B*. (*E* and *F*) Relative expression levels at different time points after LPS stimulation using primers targeting isoforms of LUCAT1 from *B* in THP-1 cells (*E*) and moDCs (*F*) were measured by qRT-PCR. Data are from three independent experiments in *E* or three different healthy donors in *F* (n = 3). Primer locations relative to LUCAT1 isoforms are shown at the bottom. (*G–J*) Relative expression levels of LUCAT1 using primer I (*G*) and primer IV (*H*), IFNB (*I*), and IL6 (*J*) in THP-1 cells that have been transduced with an empty vector control (EV) or vectors encoding transcripts LUCAT1.1 or LUCAT1.2 have been measured by qRT-PCR. Cells have been left untreated (NT) or stimulated with 200 ng/mL LPS for 2 h. Data are from three independent experiments (n = 3). Data are represented as mean (*E* and *F*) or mean ± SEM (*G–J*). *P* values (**$P \le 0.01$, ***$P \le 0.001$) have been determined by one-way or two-way ANOVA in *G–J*. NT: not treated.

a particularly long exon #3 over 5 kilobases (kb) in length, that had not been annotated previously (Fig. 2 *B–D* and Dataset S1). We confirmed the presence of these transcripts using Quantitative Reverse Transcription PCR (qRT-PCR) with isoform-specific primers in THP-1 cells (Fig. 2*E*) and moDCs (Fig. 2*F*). We synthesized and cloned the two most abundant transcripts, LUCAT1.1 and LUCAT1.2, into a lentiviral expression plasmid for ectopic expression in THP-1 cells. Cells transduced with these vectors lead to robust expression of isoform LUCAT1.2 (Fig. 2*G*) as well as significant expression of the long isoform LUCAT1.1 despite its large size (Fig. 2*H*). We treated these cells with LPS and measured IFNβ by qRT-PCR. Only the long isoform LUCAT1.1 led to an inhibition of IFN-β after a 2-h stimulation with LPS compared to the empty vector (EV) control (Fig. 2*I*). In addition, the levels of IL-6 in LUCAT1.1 overexpressing cells showed a slight reduction but was not statistically significant (Fig. 2*J*). These studies define the regulation and expression of LUCAT1 isoforms in myeloid cells and underscore the importance of the long LUCAT1.1 isoform in the suppression of immune gene expression.

LUCAT1 Binds Nuclear Proteins Regulating mRNA Splicing and Processing. To better understand how LUCAT1 restrains immune gene expression, we performed comprehensiveidentification of RNA-binding proteins by mass spectrometry (ChIRP-MS) in THP-1 cells to define the LUCAT1 interactome. We generated biotinylated ssDNA probes that were antisense to LUCAT1, which were used to enrich LUCAT1 in THP-1 cells that were stimulated with LPS and cross-linked with formaldehyde. The antisense probes to LUCAT1 showed a significant enrichment for LUCAT1 in these cells (Fig. 3*A*). The pulldown samples were then analyzed for LUCAT1-binding proteins by mass spectrometry (Dataset S2). Among the most highly enriched proteins were many known nuclear RNA-binding proteins including several heterogeneous nuclear riboproteins (e.g., hnRNP C, U, M, A2B1, and K), RNA helicases (DHX9, DDX5, and DDX17), and the whole DNA-dependent protein kinase (DNA-PK) complex (PRKDC, XRCC5, and XRCC6) (Fig. 3 *B–D*). Notably, the most abundant proteins interacting with LUCAT1 were known to be involved in processing and splicing of mRNAs (Fig. 3 *D* and *E*). We further confirmed binding of LUCAT1 to hnRNP C and A2B1 in moDCs using RNA immunoprecipitation (RIP) followed by qPCR (Fig. 3 *F* and *G*). Even in the basal state (NT) enrichment of LUCAT1 in the pulldown of both proteins was detectable and further increased after LPS stimulation.

LUCAT1 Regulates mRNA Splicing and Stability of the Anti-Inflammatory Protein NR4A2. To determine if the interaction of LUCAT1 with splicing factors identified by ChIRP-MS affects global splicing patterns, we performed RNA-seq on stimulated and unstimulated LUCAT1-deficient THP-1 cells in comparison with non-targeting control gRNA cells (NTC) and analyzed the dataset for alternative splicing events. In line with previous results, inflammatory and IFN response genes were enriched in LUCAT1-deficient cells (*SI Appendix*, Fig. S3 *A–D* and Dataset S3). Splicing analyses revealed global changes in splicing events, with a greater

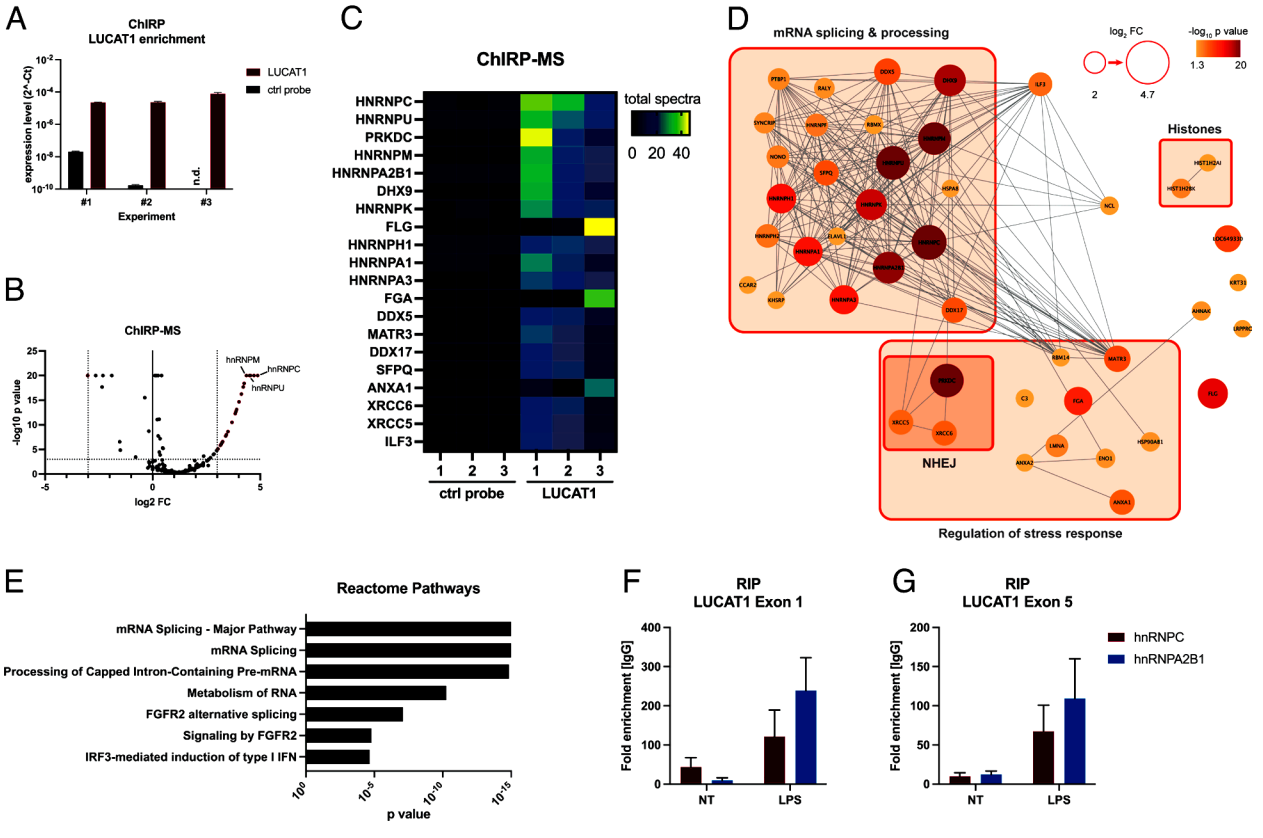

Fig. 3. LUCAT1-interacting proteins determined by ChIRP-MS. (*A*) LUCAT1 enrichment in ChIRP pulldown samples was determined by qRT-PCR for LUCAT1-binding and control probe. Data are from two technical replicates and three independent experiments in total (n = 3). (*B–D*) LUCAT1-binding proteins were determined by mass spectrometry and are presented as volcano plot (*B*), heatmap (*C*), and interaction map (*D*). Grouping of proteins in *D* is based on GO term analysis. (*E*) Reactome pathway analysis based on enriched LUCAT1-binding proteins with $\log_2$ FC ≥ 2 and p value ≤ 0.05. (*F* and *G*) LUCAT1 levels determined for RIP with hnRNP C and A2B1 relative to IgG control antibody in moDCs. LUCAT1 levels were determined by qRT-PCR for exon 1 (*F*) and exon 5 (*G*). Data are from three to four different healthy donors (n = 3 to 4). (*A*, *F*, and *G*) Data are represented as mean ± SEM. *P* values have been determined by Fisher's exact test in *B* and *D*. NT: not treated; n.d.: not detectable.

number of differential splicing events after stimulation compared to untreated cells (*SI Appendix*, Fig. S4 and Dataset S4) as well as a global pattern of increased skipped exon (SE) inclusion in LUCAT1$^{-/-}$ regardless of the stimulation (Fig. 4*A*). Among these alternatively spliced genes, we identified NR4A2 as one of the most differentially spliced gene after 1 h of LPS treatment (Fig. 4*B*), with differential splicing of exon 7 (Fig. 4*C*). NR4A2 is an anti-inflammatory protein in myeloid cells that inhibits NF-κB-driven inflammation. Similar to LUCAT1, NR4A2 is a negative feedback inhibitor that is regulated by NF-κB (20–22). We further examined enrichment of 6-mers around the retained intron (RI) and SE splicing sites, and found that recognition sites for hnRNPs C, A2B1, and K were significantly enriched, especially after 1 h of LPS stimulation (*SI Appendix*, Fig. S5). Consistently, RIP analysis for hnRNP C revealed binding to NR4A2 mRNA after LPS stimulation in moDCs (*SI Appendix*, Fig. S6). In addition, analysis of LUCAT1 and NR4A2 for potential hnRNP-binding sites demonstrated an accumulation of hnRNP C-binding sites in exon 3 of the LUCAT1 isoform 1.1, unique to this isoform, as well as in the 3' untranslated region (UTR) of NR4A2 (*SI Appendix*, Fig. S7 *A* and *B* and Dataset S5). Further, several Alu repeats were identified in exon 3 of the LUCAT1 isoform 1.1 and these repeats could serve as potential binding sites for hnRNP C (23). We then analyzed expression of NR4A2 and the ratio of both splice variants in control vs. LUCAT1-deficient THP-1 cells in a time course of LPS stimulation. As expected, IFN-β levels were increased in LUCAT1$^{-/-}$ compared to the control cells (Fig. 4*D*) and LUCAT1 was induced by LPS in the control cells (Fig. 4*E*). In LUCAT1$^{-/-}$ THP-1 cells, induction of NR4A2 expression was delayed by about 3 h and expression levels were lower compared to the control cells 2 h after stimulation (Fig. 4*F*). Furthermore, a higher abundance of the alternatively spliced isoform of NR4A2 at 1 h after stimulation was confirmed by qRT-PCR (Fig. 4*G*). Several LUCAT1-binding proteins are not only involved in alternative splicing but are also known regulators of mRNA stability in general (24–27), and the regulation of NR4A2 mRNA stability through its 3′ UTR by miRNAs has been previously described (28, 29). Thus, we also measured the stability of NR4A2 mRNA using Actinomycin D (ActD) treatment. In LUCAT1$^{-/-}$ cells, stability of NR4A2 mRNA was significantly decreased (Fig. 4*H*), whereas the stability of other immune-related genes, such as IFNβ, IRF1, and TNF, (Fig. 4 *I*–*K*), remained constant. We further generated two clonal NR4A2 knockout THP-1 lines to confirm NR4A2's role as a negative regulator of immune responses in myeloid cells. Stimulation of these cells with LPS results in an increased expression of IFNβ and IL-6 after 2 and 4 h, respectively (Fig. 4 *L* and *M*). These studies demonstrate that LUCAT1 interacts with key regulators that control the splicing of NR4A2, which in turn stabilize NR4A2 to limit immune gene expression (Fig. 4*N*).

LUCAT1 Expression Is Increased in Inflammatory Disease and Correlates with Disease Severity. Since LUCAT1 has been identified as a negative feedback inhibitor of inflammatory responses in myeloid cells, we analyzed its expression in patients with inflammatory diseases. We examined bronchoalveolar lavage (BAL) samples from patients with asthma or COPD as well as healthy control patients. In COPD patients, we observed significantly increased levels of LUCAT1, whereas LUCAT1 was elevated in asthma patients but was not statistically significant (P = 0.0768) (Fig. 5*A*). In accordance with our hypothesis of LUCAT1-regulating NR4A2 mRNA, a correlation between NR4A2 and LUCAT1 levels was detectable in the BAL samples of all tested patients (Fig. 5*B*). Since the cell composition of BAL samples can differ based on the disease status of the patient, LUCAT1 expression was analyzed relative to the abundance of neutrophils, macrophages, and lymphocytes (Fig. 5 *C*–*E*). LUCAT1 correlates with the fraction of neutrophils, negatively correlates with macrophages but does not correlate with the portion of lymphocytes. Since neutrophils in the BAL are associated with increased inflammation and exacerbations (30–32), LUCAT1 levels might serve as a sensitive indicator of disease severity and inflammatory status in these patients.

In addition, we also analyzed LUCAT1 levels in gut biopsies of patients with IBD from a large cohort from the Mount Sinai Crohn's and Colitis Registry (MSCCR) (33, 34). In this dataset, LUCAT1 expression was increased in inflamed gut biopsy samples compared to non-inflamed biopsy samples (Fig. 5*F*) and also correlated with IBD disease severity (Fig. 5*G*). LUCAT1 expression correlated with NR4A2 expression levels in IBD patients with active disease (Fig. 5*H*). We next examined the co-expression of LUCAT1 with genes from Hallmark Pathway gene sets from MSigDB (Fig. 5*I*). We found that LUCAT1 had the highest total correlation with the expression of genes of the IFN response as well as TNFA signaling via NF-κB supporting the role of LUCAT1 in regulation of IFN responses and its regulation by NF-κB in IBD. These results clearly indicate regulation of LUCAT1 in inflammatory diseases and a correlation between LUCAT1 levels and severity of disease.

Discussion

Although the importance of lncRNAs in immunity and in immune homeostasis has become increasingly apparent in the last decade (2–4), the majority of lncRNAs remain functionally uncharacterized. Here, we further elucidate the molecular function of LUCAT1, a negative regulator of immune responses in human myeloid cells (10). LUCAT1 interacts with various RNA-processing proteins, and the absence of LUCAT1 leads to changes in global splicing patterns. Among the transcripts, most affected was the anti-inflammatory protein NR4A2, which our data suggest serves as a downstream mediator of LUCAT1-dependent immune gene suppression. In addition, we show that LUCAT1 levels are increased in patients suffering from chronic inflammatory diseases like COPD and IBD.

Studying lncRNAs is challenging as most are poorly annotated, and methodologies, such as RACE and subsequent cloning of these transcripts, can be laborious and difficult, especially in cases where there are a large number of isoforms with complex regulation. Short-read RNA-sequencing methodologies are limited in their ability to define lncRNA transcripts. Our initial studies of LUCAT1 identified this lncRNA based on its differential regulation in myeloid cells activated through infection or stimulation via LPS (10). We used both RACE and cloning to examine LUCAT1 transcripts and detected several different isoforms. Using CRISPR activation, we found that forced expression of LUCAT1 led to defective induction of type I IFNs. However, ectopic expression of the cloned isoforms we had identified failed to impact these responses. Based on these different results, we hypothesized that the biologically relevant isoform of LUCAT1 had not yet been defined. In contrast, long-read sequencing by nanopore (17, 35, 36) identified an unusually long transcript that we had not detected in our prior work using RACE (10). This long LUCAT1.1 isoform was inducible in DCs and overexpression of this transcript impaired the inducible inflammatory response suggesting that this is the major isoform that is functional in these cells. This study underscores the great utility of long-read sequencing technologies

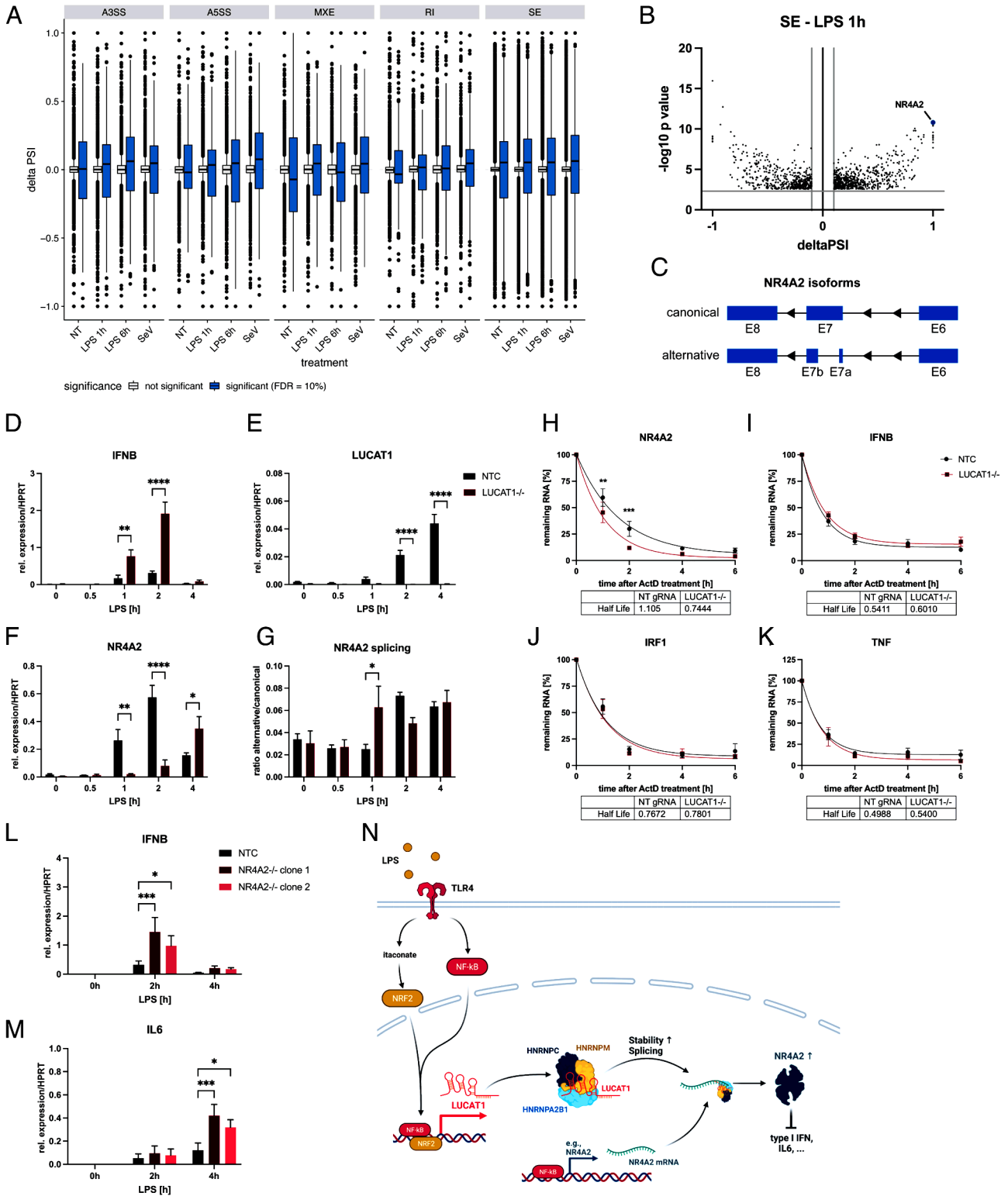

Fig. 4. LUCAT1-deficient cells demonstrate altered splicing patterns and NR4A2 levels. (*A* and *B*) Alternative splicing events in THP-1 LUCAT1$^{-/-}$ vs. control cells (non-targeting gRNA) either left untreated (NT) or stimulated with 200 ng/mL LPS for 1 h or 6 h or infected with Sendai Virus (SeV) for 6 h. Alternative splicing events A3SS (alternative 3′ splicing site), A5SS (alternative 5′ splicing site), MXE (Mutually exclusive exon), RI (retained intron), and SE are shown in *A*. Individual SE events after 1 h LPS treatment are shown in *B*. Data are from two independent experiments (n = 2). (*C*) Schematic showing alternatively spliced NR4A2 mRNA at exon 7. (*D*–*G*) Relative expression of IFNB (*D*), LUCAT1 (*E*), and NR4A2 (*F*) as well as the ratio of NR4A2 alternative to canonical transcript (*G*) in THP-1 non-targeting gRNA (NTC) and LUCAT1$^{-/-}$ cells treated for different time points with 200 ng/mL LPS. Data are from five independent experiments (n = 5). (*H*–*K*) Analysis of mRNA stability of NR4A2 (*H*), IFNB (*I*), IRF1 (*J*), and TNF (*K*) by qRT-PCR using ActD treatment for 0 to 6 h. THP-1 gRNA (NTC) and LUCAT1$^{-/-}$ cells were stimulated with 200 ng/mL LPS for 4 h before ActD was added. Data are from four independent experiments (n = 4). (*L* and *M*) Relative expression of IFNB (*L*) and IL6 (*M*) for THP-1 gRNA (NTC) and two different NR4A2$^{-/-}$ clonal cell lines (clone 1 and clone 2) was measured by qRT-PCR. Cells were left untreated (NT) or stimulated with 200 ng/mL LPS for 2 h and 4 h. Data are from three independent experiments (n = 3). (*N*) Schematic figure showing potential molecular mechanism of LUCAT1-dependent regulation of immune response. (*D*–*M*) Data are represented as mean ± SEM. *P* values (*$P \le 0.05$, **$P \le 0.01$, ***$P \le 0.001$, ****$P \le 0.0001$) were determined by two-way ANOVA in *D*–*M*. NT: not treated.

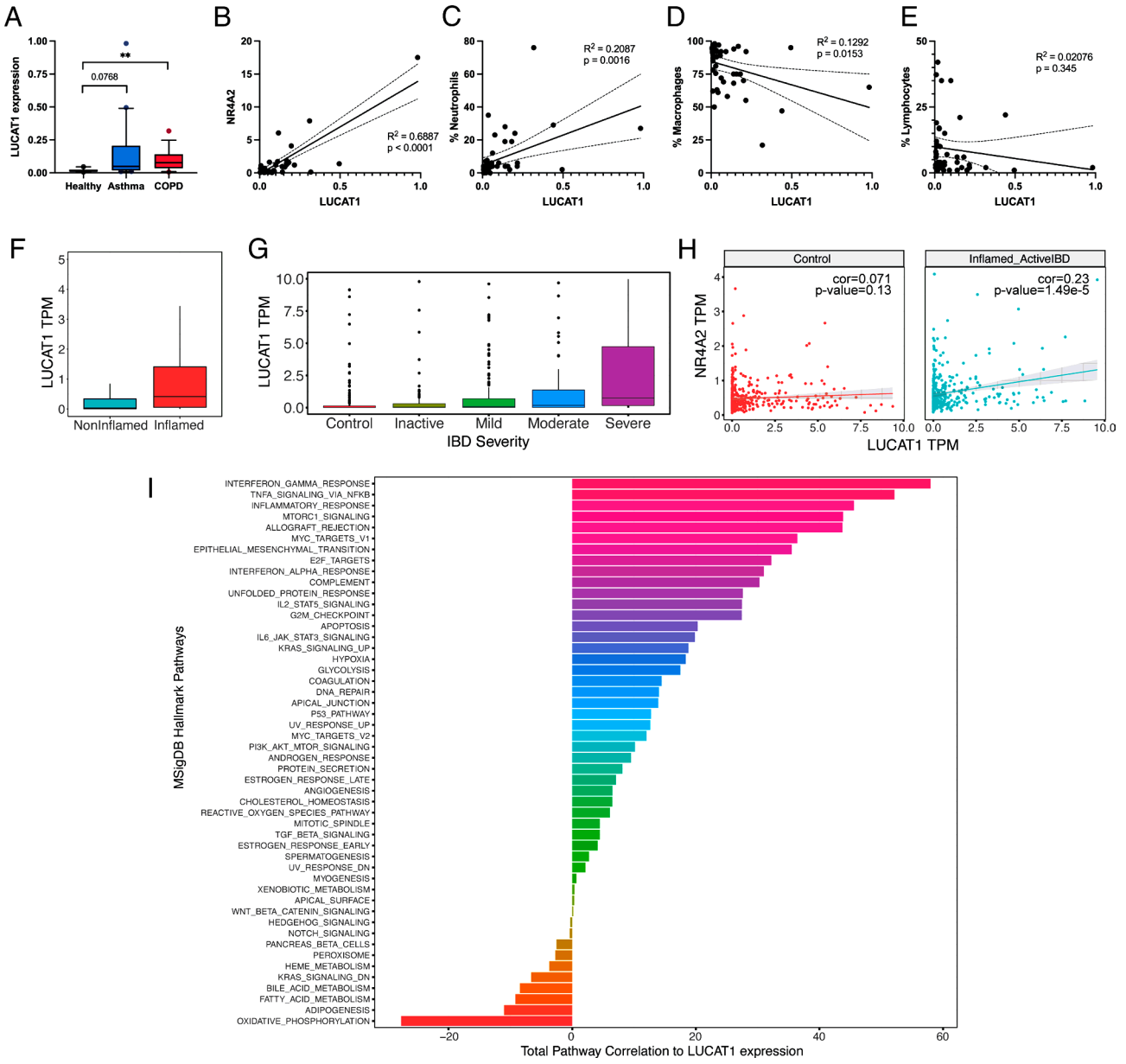

Fig. 5. LUCAT1 expression is increased in COPD and IBD and correlates with disease severity. (*A*) LUCAT1 expression in BAL samples from healthy (n = 10), asthma (n = 20), and COPD (n = 15) patients was measured by qRT-PCR. (*B–E*) Correlation of LUCAT1 levels with NR4A2 levels (*B*), fraction of neutrophils (*C*), macrophages (*D*), and lymphocytes (*E*) in BAL. (*F* and *G*) LUCAT1 expression levels shown as transcript per million (TPM) in IBD patients separated by inflamed vs. non-inflamed (*F*) or based on disease severity in *G*. (*H*) Correlation of LUCAT1 and NR4A2 in patients from non-inflamed tissue (*Left*) or active IBD (*Right*) is shown. (*I*) Total correlation of LUCAT1 expression with the gene sets from the Hallmark Pathways collection from MSigDB. Data are represented as box plot (box: median + 25 to 75 percentile; whiskers: 10 to 90 percentile) in *A* and individual points and linear regression curves are shown in *B–E*. (*A*): two-tailed Student's *t* test. $^{**}P \leq 0.01$

to define splice variants of complex genes, such as LUCAT1. Yet, we cannot exclude the possibility that other isoforms are also functional or that an interplay between different isoforms could lead to a more pronounced effect. Overexpression using CRISPRa is superior in this case as it uses the natural locus of the lncRNA and potentially induces expression of all biologically relevant splice isoforms of this gene (37), whereas usage of an expression plasmid or lentiviral expression is mostly limited to a single isoform. In addition, long transcripts, such as LUCAT1.1, also require large lentiviral transfer plasmids which results in inefficient packaging, lower yields, and less infectivity, posing additional challenges (38).

Having identified the LUCAT1.1 isoform, we next wanted to understand how LUCAT1 led to a reduction in the inducible expression of type I IFN, ISGs, and related genes. A breakthrough came from our efforts to define the LUCAT1 interactome. We found that LUCAT1 forms a ribonucleoprotein complex (RNP) with RBPs, such as hnRNPs, to affect the splicing and stability of mRNAs. Posttranscriptional regulation through these processes by lncRNA-hnRNP complexes has been previously shown for other lncRNAs, such as FIRRE (39), linc-RoR (40), and BC200 (41). The alternative splicing pattern of NR4A2 that we observed in LUCAT1$^{-/-}$ cells has also been reported to reduce NR4A2's transcriptional activity (42) and, together with the lower levels of NR4A2 mRNA, potentially leads to less biologically active NR4A2 protein. As reported previously (20–21, 22–45), deletion or knockdown of NR4A2 results in a hyperinflammatory phenotype in myeloid cells. Our study confirms these findings; yet, the elevated cytokine response in NR4A2$^{-/-}$ cells is less pronounced compared to that seen in LUCAT1$^{-/-}$ cells. This indicates that NR4A2 may not be the only mediator of LUCAT1 function. The

alternative splicing analysis revealed that global changes in splicing patterns are present that could affect other genes with immunoregulatory functions. In addition, a high-throughput analysis of mRNA stability of the whole transcriptome could identify other transcripts besides NR4A2 that are stabilized by LUCAT1. Interaction of LUCAT1 with nuclear hnRNPs could also promote the nuclear retention of LUCAT1 as shown for other lncRNAs (46, 47) in which Alu repeats play an important role. The long isoform of LUCAT1 identified in this study, LUCAT1.1, is rich in Alu repeats (*SI Appendix*, Fig. S8) which could explain its functionality and biological relevance in comparison with other isoforms.

We also found by ChIRP-MS that LUCAT1 is associated with the DNA-PK complex, consisting of the three proteins PRKDC, XRCC5, and XRCC6, which were all enriched in the LUCAT1 pulldown. DNA-PK is well known for its role as a DNA repair complex that is responsible for the repair of DNA double-strand breaks through non-homologous end joining (NHEJ) and maintaining DNA integrity (48). Moreover, the role of DNA-PK in cells is highly diverse as it can also act as an RNA-dependent protein kinase to phosphorylate hnRNP molecules (49, 50) and a recent report indicates that DNA-PK might be involved in alternative splicing of mRNAs (51). These functions could be involved in the LUCAT1-dependent splicing events that we report in this study. It is conceivable that LUCAT1 could serve as a scaffold to bring DNA-PK and hnRNPs into close proximity to promote their phosphorylation and activity. In addition, LUCAT1 has been identified as a cancer-associated lncRNA, especially in the case of lung cancer cell lines and non-small cell lung cancer (11, 52–54). Besides its role in immunosuppression, which could certainly be beneficial for cancer cells as well, LUCAT1 may regulate the DNA repair response known to depend on DNA-PK. Since mutations of PRKDC can be found in certain cancer types (55, 56) and targeting of DNA-PK is being considered as a suitable therapeutic approach in cancer (57), a better understanding of the interaction between LUCAT1 and DNA-PK in cancer cells warrants further investigation.

Overall, this study provides further insights into LUCAT1 as a negative feedback inhibitor of immune responses. Our results show that LUCAT1 participates in post-transcriptional regulation of mRNAs including NR4A2 underscoring the known role of NR4A2 as an anti-inflammatory protein and mediator of LUCAT1 function. The increased levels of LUCAT1 in patients suffering from COPD or IBD may be a result of persistent inflammation that induces LUCAT1 expression. In these diseases, LUCAT1 and the gene signature co-regulated with this lncRNA could serve as prognostic marker as it correlates with disease severity and inflammation. More studies focusing on the role of LUCAT1 in inflammatory diseases are necessary since its anti-inflammatory characteristics could be leveraged. A particularly interesting aspect of LUCAT1 relates to its expression which can be modulated by already available compounds that regulate NRF2 activity such as, 4-octyl-itaconate derivatives, or di-methyl fumarate (DMF), an FDA approved drug used therapeutically in multiple sclerosis (MS) due to its immunosuppressive characteristics (58). Hence, a better understanding of LUCAT1 biology has the potential to lead to advance targeted therapies for the treatment of inflammatory diseases.

Materials and Methods

Ethics. De-identified human blood products were obtained from the Rhode Island Blood Center. All studies were conducted with Institutional Review Board and Institutional Biosafety committee approval. All donors provided written informed consent.

moDCs and Macrophages. Peripheral blood mononuclear cells (PBMCs) were isolated from leukoreduction system (LRS) chambers using lymphoprep density gradient centrifugation (Stemcell Technologies). LRS chambers from healthy donors were obtained from the Rhode Island Blood Center. CD14+ monocytes were isolated from PBMCs by magnetic cell separation using CD14 microbeads (Miltenyi). moDCs were differentiated from CD14+ monocytes using a cocktail of IL-4 and GM-CSF (produced in 293T cells) in RPMI 1640 (Thermo) with 10% pooled human AB serum (Sigma) and 1% Pen/Strep (Thermo) for 6 to 8 d.

Cell Culture. THP-1 cells (ATCC) were cultured in RPMI 1640 (Thermo) supplemented with 10% FCS (R&D) and 1% Pen/Strep (Thermo). LUCAT1$^{-/-}$ THP-1 have been generated previously (10). Cells were differentiated into macrophage-like cells using 10 ng/mL phorbol-12-myristate acetate (PMA, Sigma) for 24 h, followed by media change and resting in PMA-free medium for another 24 h before stimulation. Cells were treated with 200 ng/mL LPS from *E. coli* 0111:B4 (Invivogen), Sendai virus Cantrell strain (Charles River Laboratories), 10 ng/mL IFN-α 2b (Gemini), 100 μM to 250 μM 4-octyl itaconate, 250 μM di-methyl itaconate, 5 μM sulforaphane (all Sigma), or 500 nM diABZI-4 (GSK) (19).

Lentivirus Production in 293T Cells and Transduction. Sequences for LUCAT1.1 and LUCAT1.2 were synthesized and cloned into LeGO-Inc backbone (addgene, # 80624) by Genewiz. LeGO-Inc was a gift from Jan-Henning Klusmann (59). Due to its length and repetitive elements, the manufacturer was only able to clone LUCAT1.1 with a 3 nt deletion (AAA at position 4,378 to 4,380 bp). Lentivirus containing either a LUCAT1 transcripts or an EV were produced in HEK 293T cells. For that purpose, 2 × 10^6 cells were seeded into 6-well plates and cultured o/n. The transfection mix was prepared in 200 μL JetPrime buffer with 10 μL JetPrime reagent (both Polyplus Transfection), 2.5 μg LeGO transfer plasmid, 1.875 μg psPAX2 (addgene, #12260), and 0.625 μg pMD2 (addgene, #12259) and added to the cells. The transfection medium was replaced after 12 h with fresh medium, and after 3 d, the supernatant containing the lentiviral particles was collected. The supernatants were concentrated using Lenti-X concentrator (Takara) according to the manufacturer's instructions by factor 100 in PBS. 0.5 × 10^6 THP-1 cells were transduced with 25 μL of concentrated lentiviral supernatant with 5 μg/mL polybrene (Qiagen). After 18 h, the medium was replaced with fresh culture medium, and after another 24 h, 5 μg/mL Blasticidin (Thermo) were added for 10 d to selected successfully transduced cells.

Long-Read Nanopore Sequencing. Libraries were generated with RNA from stimulated moDC and MDMs. RNA was enriched for poly(A) RNA using NEBNext Poly(A) mRNA Magnetic Isolation Module (NEB) and libraries were prepared using direct RNA-sequencing (SQK-RNA002) or direct cDNA-sequencing (SQK-DCS109) kits (Oxford Nanopore Technologies). Libraries were sequenced with a MinION 1B device on an R9.4.1 flow cells (all Oxford Nanopore Technologies). Basecalling was performed using guppy v4.2.2 (high accuracy) on Tesla V100 gpu (Nvidia). Full-length reads were identified using pychopper v2.5.0 and filtered reads were aligned to the human genome (assembly GRCh38/hg38) using minimap2 v2.17 with the parameters "-ax splice -uf -k14." Annotations were generated using Stringtie v2.1.5 with the parameters "-g 200 -L –conservative" based on the aligned reads and supported by Gencode annotation v38. Aligned reads and annotations were visualized using IGV v2.9.4.

qRT-PCR. RNA was isolated using Aurum total RNA mini kit (Bio-Rad). RNA was reverse transcribed using iScript Reverse Transcription Supermix (Bio-Rad). Quantitative PCR was performed using iTaq Universal SYBR Green Supermix on a C1000 Thermo Cycler (both Bio-Rad) according to the manufacturer's instructions with the following cycling conditions: 95 °C for 2 min, [95 °C for 15 s and 60 °C for 30 s] ×40 cycles followed by melting curve analysis (60 °C to 95 °C with 0.5 °C increments). Relative expression values were calculated using delta Ct method with HPRT as reference gene if not indicated otherwise. qPCR primers were purchased from Integrated DNA Technologies and are shown in *SI Appendix*, Table S1.

RNA Interference (RNAi). For gene interference in hMDMs, cells were transfected on day 6 and 8 post-isolation in 48-well plates with a pool of NRF2-specific siRNAs (sc-37030), or siRNA controls (sc-37007) at 30 nM (both Santa Cruz Biotechnology) using Lipofectamine RNAiMax (Life technologies) according to the manufacturer's instructions, followed by stimulation on day 10. HaCaT cells were transfected with 80 pM siRNA for 72 h before being processed as previously described (60).

NRF2 ChIP-seq and ChIP-qPCR. NRF2 ChIP-seq data in A549 cells have been previously published by Olagnier et al. (60) and are publicly available at GSE113522.

ChIRP-MS. ChIRP-MS has been performed as previously described (10, 61). Briefly, differentiated THP-1 wildtype cells were stimulated for 2 h with 200 ng/mL LPS and subsequently cross-linked with 3% formaldehyde for 30 min. After lysis, pulldown was performed using 3′-biotinylated probes (IDT) either specific for LUCAT1 or control probes specific for the *Drosophila melanogaster* RNA roX2 (*SI Appendix*, Table S4). Proteomic analysis of pulldown samples was performed at University of Massachusetts Chan Medical School Mass Spectrometry Facility.

RIP. RIP was performed using Magna Nuclear RIP kit (Millipore) according to the manufacturer's instructions in moDCs stimulated with 200 ng/mL LPS for 2 h or left untreated. Cells were cross-linked with 0.3% formaldehyde for 10 min after stimulation and before lysis was performed. Antibodies for hnRNPC (4F4, Thermo), hnRNP A2B1 (DP3B3, Novus Biologicals), and normal mouse IgG (12-371, Millipore) were used.

Short-Read RNA-seq and Splicing Analysis. RNA-sequencing libraries were prepared using TruSeq total RNA library prep kit with 1 µg RNA as input per sample and sequenced on a NextSeq 2000 (both Illumina) as 2× 150 bp paired end reads. Reads were processed using DolphinNext platform (62). Ribosomal RNA reads were aligned with bowtie v1.2.2 and filtered. Remaining reads were aligned to the human genome (assembly GRCh38/hg38) using STAR v2.6.1 (63), and reads were counted using RSEM v1.3.1. Differential gene expression analysis was conducted using DEBrowser v1.22.5 (64) with DeSeq2.

For alternative splicing analyses, high-throughput sequencing reads were mapped with STAR v2.7.0 (63) (default parameters) to the hg38 reference genome, guided by gene annotations from ENSEMBL hg38.v99. Alternative splicing was quantified with rMATs v4.1.0 (65), again scaffolded on the ENSEMBL hg38.v99 genome annotations, with parameters "--libType fr-firststrand --readLength 151 –variable-read-length." Within each condition (NT, LPS 1h, LPS 6h, and SeV), alternative splicing changes were assessed by comparing between the LUCAT1$^{-/-}$ replicates and gRNA replicates (NTC). Splicing events with FDR <= 10% were identified as significant.

mRNA Stability Assay. THP-1 cells were stimulated for 4 h with 200 ng/mL LPS. After stimulation, the medium was replaced with fresh culture medium containing 5 µg/mL ActD (Sigma) for 0 h to 6 h. RNA was isolated, and qRT-PCR was performed as described. For analysis, values were normalized to 0 h time point and RNA half-lives t1/2 were calculated using GraphPad v9.3.1 using nonlinear fit (one-phase decay) option.

Generation of Knockout Cell Lines Using CRISPR/Cas9. Generation of LUCAT1$^{-/-}$ THP-1 cells has been previously described (10). NR4A2$^{-/-}$ cells have been generated using the same method with two different gRNA sequences for clone 1 and clone 2 (*SI Appendix*, Table S2). To verify success of the knockout, a region of 718 bp around the gRNA cleavage sites has been amplified by PCR (*SI Appendix*, Table S3) and sequenced using Sanger sequencing at Azenta Life Sciences and frameshift mutations of 314 bp and 110 bp in the coding region of NR4A2 for clone 1 and clone 2 have been identified.

Computation of Potential hnRNP-Binding Sites. To determine potential binding sites of hnRNP C, A2B1, M, and U, RBPmap v1.2 (66) was used. Sequences for LUCAT1.1 (this study) and NR4A2 (NM_006186.4) were used as input with "high stringency" setting enabled.

Analysis of Gene Expression in BAL Cells from Asthma/COPD Patients. All subjects underwent a flexible fiberoptic bronchoscopy according to current German guidelines with intravenous (Midazolam, Propofol) and local (Lidocaine) anesthesia at the physicians' discretion (67). The bronchoscope was wedged into a subsegmental bronchus of the middle lobe and BAL was performed in 15 × 20 mL fractions of warmed sterile 0.9% sodium chloride and retrieved by gentle suction. Fractions were pooled, washed twice by centrifugation at 400 × g for 10 min with phosphate-buffered Dulbecco's saline (PAA Laboratories, Pasching, Austria), and the cell pellet stored at −80 °C until used in the analyses described here. Cell differentiation of BAL cells was determined on cytospin slides by Hemacolor staining and cell viability by trypan blue dye. BAL cells from healthy adult subjects come from the GeKo FZB study (www.DRKS.de; identifier DRKS00016932), who additionally gave written and verbal broad consent according to ICH/GCP (Good Clinical Practice) standards (EC HL Ref. 15-194; EC HL Ref. 14-225). BAL cells from adult patients are historical residual material from reserve samples that are no longer needed for diagnostics and would otherwise have been destroyed. In accordance with the vote of the Ethics Committee of the University of Lübeck (EC HL Ref. 12-220), these samples were included anonymously. The biospecimens and data used in the present study were issued on the basis of a project-specific sample and data use application including an ethics vote in accordance with the regulations of the BioMaterialBank Nord (EK HL Ref. 21-446).

Patient information is shown in *SI Appendix*, Table S5. RNA from BAL cells was isolated using innuPREP RNA Mini Kit 2.0 (Analytik Jena). Using the same amount of total RNA for every sample, reverse transcription was performed using Superscript III and Oligo(dT)12-18 (ThermoFisher). qPCR was carried out with the LightCycler® 480 SYBR Green I Master (Roche) using following protocol: initial denaturation at 95 °C for 5 min followed by 45 cycles of denaturation at 95 °C for 10 s, annealing starting at 63 °C and ending with 58 °C (0.5 °C increasement) for 5 s, and extension at 72 °C for 6 s. After the last cycle, a final denaturation step at 95 °C for 1 min was performed followed by cooling down to 40 °C in 30 s. qRT-PCR was carried out on LightCycler 480 II instrument and analyzed by LightCycler 480 SW 1.5.1 software (both Roche). For BAL samples, TBP was used as a reference gene.

Analysis of IBD Dataset. The dataset used in this study was the MSCCR of biopsy whole transcriptome-sequencing data from a cross-sectional cohort composed of 1,170 patients enrolled in the MSCCR from December 2013 to September 2016. The protocol was approved by the Icahn School of Medicine at Mount Sinai IRB (33, 34). The fastq files were trimmed with cutadapt using the options "-a AGATCGGAAGAGCACACGTCTGAACTCCAGTCA –minimum-length 1 -j 15" (68). The trimmed fastq files were pseudoaligned and quantified using Salmon version 1.5.2 using a custom reference genome composed of Lncipedia 5.2 high confidence lncRNAs combined with protein-coding genes from GENCODE release 38 (GRCh38.p13) (69, 70). Salmon results files were imported into R using the package tximeta Bioconductor release 3.14 (71). Gene-level counts were generated using the function summarizeToGene and TPM-normalized. To examine the correlation of LUCAT1 expression with genes in the MSigDB Hallmark Pathways, the correlation of LUCAT1 to every gene in a particular pathway was calculated. The sum of all the gene correlations for a pathway was then taken as the total pathway correlation.

Statistical Analysis. The data were analyzed for statistical significance using a one-way or two-way ANOVA or two-tailed Student's *t* test in Graph Pad Prism 9.3.1 software. Values of $P \leq 0.05$ were considered to be statistically significant.

Data, Materials, and Software Availability. RNA sequencing data are deposited in GEO under the primary accession code GSE202409 (72).

ACKNOWLEDGEMENTS. This work is supported by a research fellowship from the German Research Foundation (DFG, VI 1027/1-1 to T.V.) by grants from the NIH (AI067497, AI147208 and AI142231 to K.A.F.) and by a sponsored research grant from Janssen Research & Development, LLC to K.A.F.). We thank Steffi Fox and Margrit Kernbach from the BioMaterial Bank Nord for their technical assistance and Rainer Vogler for medical documentation. The BioMaterialBank Nord is supported by the German Centre for Lung Research (DZL) and member of popgen 2.0 network (P2N), which is supported by a grant from the German Ministry for Education and Research (grant number: 01EY1103). This work was completed in part with resources provided by the University of Massachusetts' Green High Performance Computing Cluster (GHPCC).

Author affiliations: [a]Division of Innate Immunity, University of Massachusetts Chan Medical School, Worcester, MA 01605; [b]Janssen R&D, Discovery, Spring House, PA 19002; [c]Division of Innate Immunity, Research Center Borstel–Leibniz Lung Center, Borstel 23845, Germany; [d]German Center for Lung Research, Airway Research Center North, Borstel 23845, Germany; [e]Department of Biomedicine, Aarhus University, Aarhus 8000,

Denmark; [f]BioMaterialBank North, Research Center Borstel–Leibniz Lung Center, Borstel 23845, Germany; [g]Center for Clinical Studies, Research Center Borstel–Leibniz Lung Center, Borstel 23845, Germany; [h]RNA Therapeutics Institute, University of Massachusetts Chan Medical School, Worcester, MA 01605; and [i]Bristol Myers Squibb, Immunology Cardiovascular and Fibrosis Translational Early Development, Summit, NJ 07901

Author contributions: T.V., S.A., J.L.J., X.L., D.O., A.P., A.O., K.H., and K.A.F. designed research; T.V., S.A., J.L.J., L.G., X.L., K.S., D.O., K.I.G., C.H., and A.P. performed research; D.O., K.I.G., C.H., C.H.K., H.H., A.P., and A.O. contributed new reagents/analytic tools; T.V., S.A., J.L.J., X.L., K.S., C.H.K., H.H., A.P., K.H., and K.A.F. analyzed data; and T.V., J.L.J., A.O., and K.A.F. wrote the paper.

1. W. K. Mowel, J. J. Kotzin, S. J. McCright, V. D. Neal, J. Henao-Mejia, Control of immune cell homeostasis and function by lncRNAs. *Trends Immunol.* **39**, 55–69 (2018).
2. F. Agliano, V. A. Rathinam, A. E. Medvedev, S. K. Vanaja, A. T. Vella, Long noncoding RNAs in host-pathogen interactions. *Trends Immunol.* **40**, 492–510 (2019).
3. T. Vierbuchen, K. A. Fitzgerald, Long non-coding RNAs in antiviral immunity. *Semin. Cell Dev. Biol.* **111**, 126–134 (2021).
4. K. Walther, L. N. Schulte, The role of lncRNAs in innate immunity and inflammation. *RNA Biol* **18**, 587–603 (2021).
5. J. J. Quinn, H. Y. Chang, Unique features of long non-coding RNA biogenesis and function. *Nat. Rev. Genet* **17**, 47–62 (2016).
6. S. Carpenter *et al.*, A long noncoding RNA mediates both activation and repression of immune response genes. *Science* **341**, 789–792 (2013).
7. Q. Zhang *et al.*, The long noncoding RNA ROCKI regulates inflammatory gene expression. *EMBO J.* **38**, e100041 (2019).
8. J. J. Kotzin *et al.*, The long non-coding RNA Morrbid regulates Bim and short-lived myeloid cell lifespan. *Nature* **537**, 239–243 (2016).
9. M. Aznaourova *et al.*, Noncoding RNA MaIL1 is an integral component of the TLR4-TRIF pathway. *Proc. Natl. Acad. Sci. U.S.A.* **117**, 9042–9053 (2020).
10. S. Agarwal *et al.*, The long non-coding RNA LUCAT1 is a negative feedback regulator of interferon responses in humans. *Nat. Commun.* **11**, 6348 (2020).
11. P. Thai *et al.*, Characterization of a novel long noncoding RNA, SCAL1, induced by cigarette smoke and elevated in lung cancer cell lines. *Am. J. Res. Cell Mol. Biol.* **49**, 204–211 (2013).
12. L. A. J. O'Neill, M. N. Artyomov, Itaconate: The poster child of metabolic reprogramming in macrophage function. *Nat. Rev. Immunol.* **19**, 273–281 (2019).
13. E. L. Mills *et al.*, Itaconate is an anti-inflammatory metabolite that activates Nrf2 via alkylation of KEAP1. *Nature* **556**, 113–117 (2018).
14. D. G. Ryan *et al.*, Nrf2 activation reprograms macrophage intermediary metabolism and suppresses the type I interferon response. *iScience* **25**, 103827 (2022).
15. M. Bambouskova *et al.*, Electrophilic properties of itaconate and derivatives regulate the IkappaBzeta-ATF3 inflammatory axis. *Nature* **556**, 501–504 (2018).
16. J. Muri, H. Wolleb, P. Broz, E. M. Carreira, M. Kopf, Electrophilic Nrf2 activators and itaconate inhibit inflammation at low dose and promote IL-1beta production and inflammatory apoptosis at high dose. *Redox Biol.* **36**, 101647 (2020).
17. A. C. Vollmers, H. E. Mekonen, S. Campos, S. Carpenter, C. Vollmers, Generation of an isoform-level transcriptome atlas of macrophage activation. *J. Biol. Chem.* **296**, 100784 (2021).
18. R. De Paoli-Iseppi, J. Gleeson, M. B. Clark, Isoform age–Splice isoform profiling using long-read technologies. *Front Mol. Biosci.* **8**, 711733 (2021).
19. F. Humphries *et al.*, A diamidobenzimidazole STING agonist protects against SARS-CoV-2 infection. *Sci. Immunol.* **6**, eabi9002 (2021).
20. K. Saijo *et al.*, A Nurr1/CoREST pathway in microglia and astrocytes protects dopaminergic neurons from inflammation-induced death. *Cell* **137**, 47–59 (2009).
21. S. Mahajan *et al.*, Nuclear receptor Nr4a2 promotes alternative polarization of macrophages and confers protection in sepsis. *J. Biol. Chem.* **290**, 18304–18314 (2015).
22. C. McEvoy *et al.*, NR4A receptors differentially regulate NF-kappaB signaling in myeloid cells. *Front Immunol.* **8**, 7 (2017).
23. K. Zarnack *et al.*, Direct competition between hnRNP C and U2AF65 protects the transcriptome from the exonization of Alu elements. *Cell* **152**, 453–466 (2013).
24. L. E. Rajagopalan, C. J. Westmark, J. A. Jarzembowski, J. S. Malter, hnRNP C increases amyloid precursor protein (APP) production by stabilizing APP mRNA. *Nucleic Acids Res.* **26**, 3418–3423 (1998).
25. M. Yugami, Y. Kabe, Y. Yamaguchi, T. Wada, H. Handa, hnRNP-U enhances the expression of specific genes by stabilizing mRNA. *FEBS Lett.* **581**, 1–7 (2007).
26. F. Jiang *et al.*, HNRNPA2B1 promotes multiple myeloma progression by increasing AKT3 expression via m6A-dependent stabilization of ILF3 mRNA. *J. Hematol. Oncol.* **14**, 54 (2021).
27. P. Hou *et al.*, LINC00460/DHX9/IGF2BP2 complex promotes colorectal cancer proliferation and metastasis by mediating HMGA1 mRNA stability depending on m6A modification. *J. Exp. Clin. Cancer Res.* **40**, 52 (2021).
28. L. A. Pereira, R. Munita, M. P. González, M. E. Andrés, Long 3'UTR of Nurr1 mRNAs is targeted by miRNAs in mesencephalic dopamine neurons. *PLOS One* **12**, e0188177 (2017).
29. J. A. Beard *et al.*, The orphan nuclear receptor NR4A2 is part of a p53-microRNA-34 network. *Sci. Rep.* **6**, 25108 (2016).
30. D. Stanescu *et al.*, Airways obstruction, chronic expectoration, and rapid decline of FEV1 in smokers are associated with increased levels of sputum neutrophils. *Thorax* **51**, 267–271 (1996).
31. R. O'Donnell, D. Breen, S. Wilson, R. Djukanovic, Inflammatory cells in the airways in COPD. *Thorax* **61**, 448–454 (2006).
32. A. Herrero-Cervera, O. Soehnlein, E. Kenne, Neutrophils in chronic inflammatory diseases. *Cell Mol. Immunol.* **19**, 177–191 (2022).
33. M. Suárez-Fariñas *et al.*, INtestinal inflammation modulates the expression of ACE2 and TMPRSS2 and potentially overlaps with the pathogenesis of SARS-CoV-2-related disease. *Gastroenterology* **160**, 287–301.e220 (2021).
34. C. Argmann *et al.*, Molecular characterization of limited ulcerative colitis reveals novel biology and predictors of disease extension. *Gastroenterology* **161**, 1953–1968.e1915 (2021).
35. C. Soneson *et al.*, A comprehensive examination of Nanopore native RNA sequencing for characterization of complex transcriptomes. *Nat. Commun.* **10**, 3359 (2019).
36. R. E. Workman *et al.*, Nanopore native RNA sequencing of a human poly(A) transcriptome. *Nat. Methods* **16**, 1297–1305 (2019).
37. S. Konermann *et al.*, Genome-scale transcriptional activation by an engineered CRISPR-Cas9 complex. *Nature* **517**, 583–588 (2015).
38. N. P. Sweeney, C. A. Vink, The impact of lentiviral vector genome size and producer cell genomic to gag-pol mRNA ratios on packaging efficiency and titre. *Mol. Ther. Methods Clin. Dev.* **21**, 574–584 (2021).
39. Y. Lu *et al.*, The NF-kappaB-responsive long noncoding rna firre regulates posttranscriptional regulation of inflammatory gene expression through interacting with hnRNPU. *J. Immunol.* **199**, 3571–3582 (2017).
40. J. Huang *et al.*, Linc-RoR promotes c-Myc expression through hnRNP I and AUF1. *Nucleic Acids Res.* **44**, 3059–3069 (2016).
41. R. Singh *et al.*, Regulation of alternative splicing of Bcl-x by BC200 contributes to breast cancer pathogenesis. *Cell Death Dis.* **7**, e2262 (2016).
42. S. K. Michelhaugh *et al.*, Dopamine neurons express multiple isoforms of the nuclear receptor nurr1 with diminished transcriptional activity. *J. Neurochem.* **95**, 1342–1350 (2005).
43. D. Crean *et al.*, Adenosine modulates NR4A orphan nuclear receptors to attenuate hyperinflammatory responses in monocytic cells. *J. Immunol.* **195**, 1436–1448 (2015).
44. K. A. Popichak *et al.*, Compensatory expression of nur77 and nurr1 regulates NF-kappaB-dependent inflammatory signaling in astrocytes. *Mol. Pharmacol.* **94**, 1174–1186 (2018).
45. W. Liu, Y. Gao, N. Chang, Nurr1 overexpression exerts neuroprotective and anti-inflammatory roles via down-regulating CCL2 expression in both in vivo and in vitro Parkinson's disease models. *Biochem. Biophys. Res. Commun.* **482**, 1312–1319 (2017).
46. E. Hacisuleyman, C. J. Shukla, C. L. Weiner, J. L. Rinn, Function and evolution of local repeats in the Firre locus. *Nat. Commun.* **7**, 11021 (2016).
47. Y. Lubelsky, I. Ulitsky, Sequences enriched in Alu repeats drive nuclear localization of long RNAs in human cells. *Nature* **555**, 107–111 (2018).
48. A. J. Davis, B. P. Chen, D. J. Chen, DNA-PK: A dynamic enzyme in a versatile DSB repair pathway. *DNA Repair (Amst)* **17**, 21–29 (2014).
49. S. Zhang, B. Schlott, M. Gorlach, F. Grosse, DNA-dependent protein kinase (DNA-PK) phosphorylates nuclear DNA helicase II/RNA helicase A and hnRNP proteins in an RNA-dependent manner. *Nucleic Acids Res.* **32**, 1–10 (2004).
50. A. Anisenko, M. Kan, O. Shadrina, A. Brattseva, M. Gottikh, Phosphorylation targets of DNA-PK and their role in HIV-1 replication. *Cells* **9**, 1907 (2020).
51. Z. Song *et al.*, Genome-wide identification of DNA-PKcs-associated RNAs by RIP-Seq. *Signal Transduct. Target Ther.* **4**, 22 (2019).
52. Y. Sun *et al.*, Long non-coding RNA LUCAT1 is associated with poor prognosis in human non-small lung cancer and regulates cell proliferation via epigenetically repressing p21 and p57 expression. *Oncotarget* **8**, 28297–28311 (2017).
53. B. Luzon-Toro *et al.*, LncRNA LUCAT1 as a novel prognostic biomarker for patients with papillary thyroid cancer. *Sci. Rep.* **9**, 14374 (2019).
54. C. R. V. Cruz, J. L. M. Ferrer, R. L. Garcia, Concomitant and decoupled effects of cigarette smoke and SCAL1 upregulation on oncogenic phenotypes and ROS detoxification in lung adenocarcinoma cells. *Sci. Rep.* **11**, 18345 (2021).
55. X. Wang *et al.*, Mutational analysis of thirty-two double-strand DNA break repair genes in breast and pancreatic cancers. *Cancer Res.* **68**, 971–975 (2008).
56. T. K. Er *et al.*, Targeted next-generation sequencing for molecular diagnosis of endometriosis-associated ovarian cancer. *J. Mol. Med. (Berl)* **94**, 835–847 (2016).
57. I. S. Mohiuddin, M. H. Kang, DNA-PK as an emerging therapeutic target in cancer. *Front Oncol* **9**, 635 (2019).
58. A. Hammer *et al.*, The NRF2 pathway as potential biomarker for dimethyl fumarate treatment in multiple sclerosis. *Ann. Clin. Transl. Neurol.* **5**, 668–676 (2018).
59. S. Emmrich *et al.*, LincRNAs MONC and MIR100HG act as oncogenes in acute megakaryoblastic leukemia. *Mol. Cancer* **13**, 171 (2014).
60. D. Olagnier *et al.*, Nrf2 negatively regulates STING indicating a link between antiviral sensing and metabolic reprogramming. *Nat. Commun.* **9**, 3506 (2018).
61. C. Chu, H. Y. Chang, ChIRP-MS: RNA-directed proteomic discovery. *Methods Mol Biol* **1861**, 37–45 (2018).
62. O. Yukselen, O. Turkyilmaz, A. R. Ozturk, M. Garber, A. Kucukural, DolphinNext: A distributed data processing platform for high throughput genomics. *BMC Genomics* **21**, 310 (2020).
63. A. Dobin *et al.*, STAR: Ultrafast universal RNA-seq aligner. *Bioinformatics* **29**, 15–21 (2013).
64. A. Kucukural, O. Yukselen, D. M. Ozata, M. J. Moore, M. Garber, DEBrowser: Interactive differential expression analysis and visualization tool for count data. *BMC Genomics* **20**, 6 (2019).
65. S. Shen *et al.*, rMATS: Robust and flexible detection of differential alternative splicing from replicate RNA-Seq data. *Proc. Natl. Acad. Sci. U.S.A.* **111**, E5593–5601 (2014).
66. I. Paz, I. Kosti, M. Ares Jr., M. Cline, Y. Mandel-Gutfreund, RBPmap: A web server for mapping binding sites of RNA-binding proteins. *Nucleic Acids Res.* **42**, W361–367 (2014).
67. K. Häussinger *et al.*, Recommendations for quality standards in bronchoscopy. *Pneumologie* **58**, 344–356 (2004).
68. M. Martin, Cutadapt removes adapter sequences from high-throughput sequencing reads. *EMBnet J.* **17**, 3 (2011).
69. R. Patro, G. Duggal, M. I. Love, R. A. Irizarry, C. Kingsford, Salmon provides fast and bias-aware quantification of transcript expression. *Nat. Methods* **14**, 417–419 (2017).
70. P.-J. Volders *et al.*, LNCipedia 5: Towards a reference set of human long non-coding RNAs. *Nucleic Acids Res.* **47**, D135–D139 (2018).
71. M. I. Love *et al.*, Tximeta: Reference sequence checksums for provenance identification in RNA-seq. *PLOS Comput. Biol.* **16**, e1007664 (2020).
72. K. A. Fitzgerald, Effect of LUCAT1 depletion in THP-1 monocytes on gene expression. (2022) GEO https://www.ncbi.nlm.nih.gov/geo/query/acc.cgi?acc=GSE202409) May 06, 2022.